https://doi.org/10.5194/tc-2021-259
Preprint. Discussion started: 30 August 2021
© Author(s) 2021. CC BY 4.0 License.

The Cryosphere Discussions

Melt probabilities and surface temperature trends on the Greenland ice sheet using a Gaussian mixture model

Daniel Clarkson[1], Emma Eastoe[1], and Amber Leeson[1]

[1]Lancaster University

Correspondence: Daniel Clarkson (d.clarkson@lancaster.ac.uk)

Abstract. The Greenland ice sheet has experienced significant melt over the past six decades, with extreme melt events covering large areas of the ice sheet. Melt events are typically analysed using summary statistics, but the nature and characteristics of the events themselves are less frequently analysed. Our work examines melt events from a statistical perspective by modelling 19 years of Moderate Resolution Imaging Spectroradiometer (MODIS) ice surface temperature data using a Gaussian mixture model. We use a mixture model with separate model components for ice and meltwater temperatures at 1139 locations spaced across the ice sheet. By considering the uncertainty of the ice surface temperature measurements, we use the two categories of model components to define a probability of melt for a given observation rather than using a fixed melt threshold. This probability can then be used to estimate the expected number of melt events at a given location. Furthermore, the model can be used to estimate temperature quantiles at a given location, and analyse temperature and melt trends over time by fitting the model to subsets of time. Fitting the model to data from 2001-2009 and 2010-2019 shows increases in melt probability for significant portions of the ice sheet, as well as the yearly expected maximum temperatures.

1 Introduction

The Greenland ice sheet has experienced significant melt over the past six decades (Fettweis et al., 2011) and has had an overall accelerating contribution to sea-level rise from a combination of melt and dynamical discharge, in particular over the last 18 years (Rignot et al., 2018). Wide regions of the ice sheet have lost mass over the last two decades resulting in an increasing contribution to sea-level rise (Mouginot et al., 2019). Combined with melt from other ice bodies, e.g. the Antarctic ice sheet and valley glaciers, groundwater depletion, and thermal expansion of the oceans, total sea-level rise has been far above the historical rate of sea-level rise during this period (Chen et al., 2017). Understanding where, when, and how frequently melt occurs on the Greenland ice sheet is a key part of understanding its role in sea-level rise and how we might expect it to change in the future.

Since air temperature is a strong control on ice melt (Vermeer and Rahmstorf, 2009), temperature data is often used as a proxy for melting. Ice surface temperatures exceeding $-1°C$ can be interpreted as evidence of melt depending on the dataset used and its accuracy and uncertainty (Nghiem et al., 2012). There are many ways to study the temperature of the ice sheet, including through observations from space (Zhengming and Dozier, 1989), Automatic Weather Stations (AWSs) (Tedesco et al., 2013), and using models e.g. Global Climate Models (GCMs) (Smith et al., 2007). In terms of observations, data from these diverse

https://doi.org/10.5194/tc-2021-259
Preprint. Discussion started: 30 August 2021
© Author(s) 2021. CC BY 4.0 License.


sources are characterised by differing levels of accuracy and coverage. Whilst in-situ observations are often considered to provide the most accurate measurements for a given location, and GCMs output allows consideration of temperatures under different climate scenarios, satellite data has comparable accuracy to in-situ measurements (Hall et al., 2008) with far higher spatial coverage, providing the most comprehensive overall view of the ice sheet.

In 2012, a record-breaking melt event was observed during mid-July, with 98.6% of the ice-sheet simultaneously experiencing melt (Hanna et al., 2014). Extreme melt events are likely to become more common as overall temperatures on the Greenland ice sheet increase, contributing to increasing amounts of melt. Despite their role in the overall view of melt on the ice sheet, the magnitude, frequency, and melt contribution of these melt events and future events are not clearly defined. Because these events are rare, our understanding of them has necessarily been based on observations of few isolated examples to date. Modelling these events allows us to deepen our understanding of their characteristics and drivers and to better quantify melt on the ice sheet overall.

Here, we propose a novel statistical approach applied to Moderate Resolution Imaging Spectroradiometer (MODIS) Ice Surface Temperature (IST) data to model the distribution of temperatures on the Greenland ice sheet at 1139 MODIS pixels, with a particular interest in identifying and modelling melt temperatures. The approach is based on three key characteristics of IST data: firstly, the presence of physical bounds on the range of ice and ice-melt temperatures; secondly, the multi-modality of the distribution; and thirdly, ambiguity about whether measurements close to 0°C represent melting of the ice sheet surface. Our model is sufficiently generalise-able as to be useful for pixels not explicitly used to generate the model, regardless of elevation, distance from the coast, or location, as demonstrated by the well-distributed range of pixels used for the modelling. We use this model to investigate time trends in the observation period and to quantify both the frequency and magnitude of temperature events that are likely to result in ice melt.

2 Data and methods

2.1 MODIS IST data

We use MODIS IST data from MODIS/Terra Sea Ice Extent 5-Min L2 Swath 1km, Version 6 (MOD29) contained within a multilayer Greenland MODIS-based product (Hall and DiGirolamo, 2019). MODIS records surface reflectance from 36 spectral bands of different wavelengths - including those used in IST - daily for the entire Earth. The dataset spans the period 01/03/2000 to 31/12/2019 and has a spatial resolution of .78 km $\times$ .78 km. Here we discard the first 10 months of the data set, up to 01/01/2001, in order to work only with those years for which a full annual cycle is available. To reduce the computational burden of our model, we also subsample the data taking 1 in every 50 points in both x and y dimensions for a total of 1139 points, roughly equally spaced across in latitude and longitude and thus covering a range of glaciological and climatological settings across the ice sheet.

The IST measurements represent the temperature at the surface of the ice in cloud-free conditions. Clouds (specifically water vapour) can interfere with the measurements, so a cloud mask is used in the MODIS product to remove measurements made

https://doi.org/10.5194/tc-2021-259
Preprint. Discussion started: 30 August 2021
© Author(s) 2021. CC BY 4.0 License.

The Cryosphere Discussions
Open Access
EGU

in cloudy conditions. This may induce a slight bias in the dataset since cloudy days are on average warmer than clear days (Koenig and Hall, 2010), and as a result, our analysis reflects clear conditions only.

As a result of cloud masking, areas on the coast and in the north have a higher proportion of missing data than more central areas (Figure 1). We also see that winter months have more missing data on average than summer months, with a range of 65.1% of data available in December compared to 91.1% of data available in May. This is important to bear in mind when interpreting the predictions made from the statistical models, as the IST distributions will be more heavily weighted towards warmer temperatures. This shouldn't affect our inference with regards to melt, however, as melt temperatures almost exclusively occur in the summer months which have a much lower proportion of missing data.

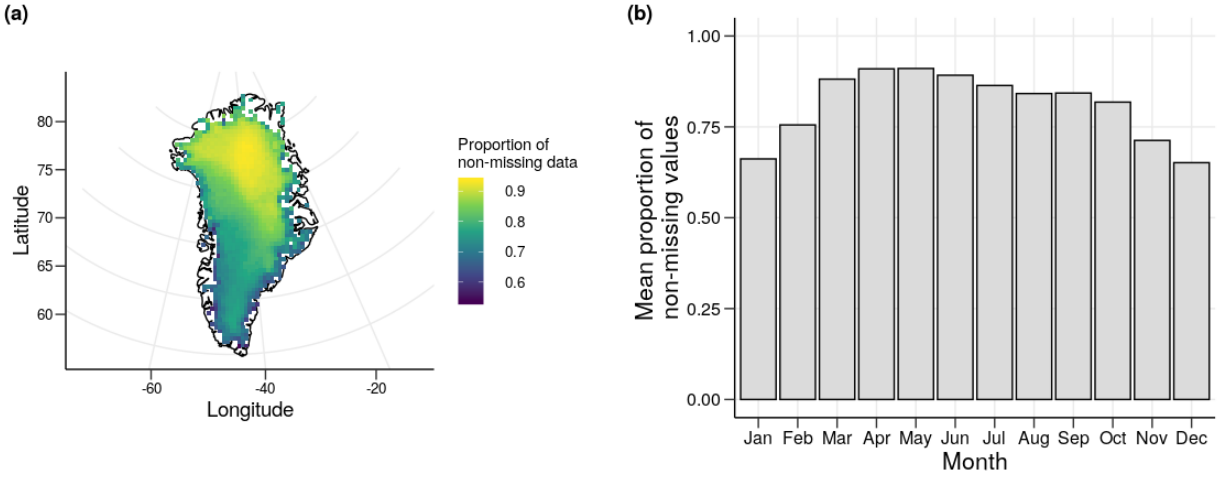

Figure 1. Proportion of non-missing MODIS IST data (i.e not filtered by the cloud mask) at 1139 locations on the Greenland ice sheet between 2001 and 2019 (a) and mean proportion of non-missing MODIS IST data by month between 2001 to 2019 (b).

2.2 Modelling considerations

To create a statistical model that is parsimonious and applicable across sites with widely varying geophysical characteristics, we model the IST data using statistical methods that allow us to treat melting in a probabilistic manner. Exploratory data analysis shows that there is no clear point in the temperature distribution that can be attributed to the onset of melting (Figure 2). As a result, we model melting ice temperatures and non-melting ice temperatures separately and estimate the probability of melt occurring over a range of temperatures. This approach allows for some uncertainty in the observations from factors such as the precision of the dataset, which has a stated uncertainty of $\pm 1^{\circ}$C). We hereby refer to temperatures associated with melting ice as "melt" temperatures and temperatures associated with non-melting ice as "ice" temperatures.

A key feature of the dataset and a core modelling consideration is the soft upper limit at 0°C. The melting point of the ice acts as a physical upper limit on ISTs, as once the ice exceeds this temperature it melts and may no longer form the surface of the ice sheet. Some sites have measurements above this limit, which arise due to meltwater sitting on top of the ice. However,

https://doi.org/10.5194/tc-2021-259
Preprint. Discussion started: 30 August 2021
© Author(s) 2021. CC BY 4.0 License.

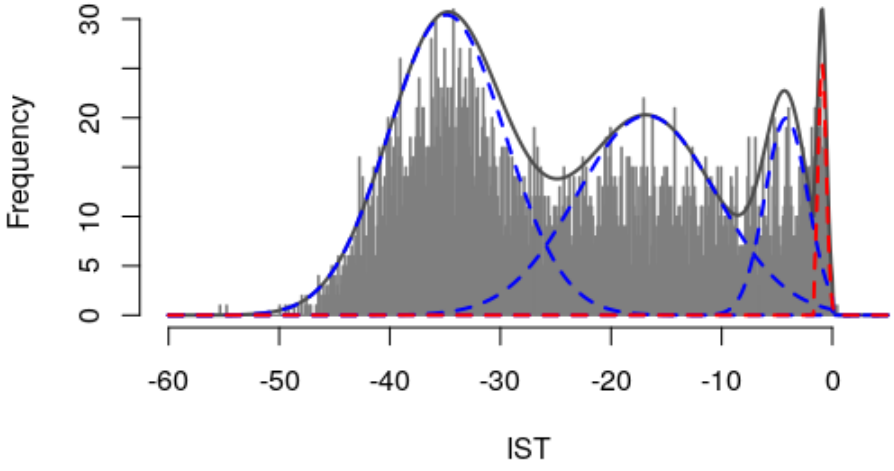

Figure 2. Frequency distribution of daily MODIS IST data from an example location (82.47, -37.50) on the Greenland ice sheet between 2001 and 2019. Solid lines show a mixture model fit to these data where black indicates the full model, blue indicates the 'ice' component and red indicates the 'melt' component.

the ice under the water places a limit on these melt temperatures, hence the distribution of positive temperatures is truncated close to $0°$C. This soft upper limit of ISTs causes a significant peak in the distribution centred at approximately $-0.5°$C, as any ISTs that would exceed $0°$C are truncated to small positive values close to $0°$C.

Furthermore, ISTs generally have a multi-modal distribution that does not follow a particular standard model e.g. Gaussian or Weibull (Figure 2). The number of modes, and their characteristics, both vary significantly from location to location, making it difficult to generalise in space using a single distribution. However, there are some consistencies in the general shape of each of the modes at different locations and the position of the distribution relative to positive temperature values. This gives us a basic set of assumptions to base our modelling around that allow the model to retain the same underlying structure regardless of the absolute difference in ISTs between locations.

2.3 Model description

In order to accommodate spatial variability in the temperature distribution, we model IST using a truncated Gaussian mixture model in which components are assigned to model groups of temperatures that we assign to be either ice or melt. For n_I ice components and a single melt component, let ϕ_i be the weight associated with model component i such that for $n_c = n_I + 1$ total components, $\sum_{i=1}^{n_c} \phi_i = 1$. For each ice component i (and melt component M) let $f_i(x)$ be the probability density function

https://doi.org/10.5194/tc-2021-259
Preprint. Discussion started: 30 August 2021
© Author(s) 2021. CC BY 4.0 License.


of the truncated normal distribution $X \sim TN(\mu_i, \sigma_i^2, a_i, b_i)$, where μ_i is the mean, σ_i is the standard deviation, a_i (b_i) is the lower (upper) truncation point. Then the probability density function of ISTs x is:

$$p(x) = \sum_{i=1}^{n_I} \phi_i f_i(x) + \phi_M f_M(x).$$

We set the upper and lower truncation points for the ice and melt components at values that bound each measurement type with relative certainty. For the ice components, $a = -\infty$ as there is no hard lower limit on the temperature of ice (aside from absolute zero), and $b = 0$ as, theoretically, ice temperature can't exceed $0°$C. This means that there is no limit on how low ice temperatures can go, but they can't exceed $0°$C. For the melt component, $b = \infty$ and $a = -1.65$, so that temperatures in the melt component can't go below $-1.65°$C but are not upper truncated. We take a bound lower than zero here to account for uncertainty in the data and any potential impurities in the ice surface. $-1.65°$C is the theoretical minimum temperature at which saline ice can melt (Hall et al., 2004), and thus should be a conservative estimate for this lower bound. Temperatures between $-1.65°$C and $0°$C can be modelled by either/both the ice and melt components as there is uncertainty as to whether they are associated with melting or non-melting ice.

A mixture model was fitted using the Expectation-Maximisation (EM) algorithm for each sample location. The algorithm alternates between two main steps: calculating the component probabilities that each observation x_i comes from model component k, and maximising the expectations of the model parameters using the component probabilities (for full details see Appendix A). We used this method to obtain estimates of μ, σ, and ϕ for each model component at each location.

We used Bayesian Information Criterion (BIC) to assess the most appropriate number of ice and melt components and found that three ice components and one melt component fit the data best. These components may be broadly interpreted as winter, autumn, spring, and the melt season for the three ice components and single melt component respectively.

When modelled with separate Gaussian components, the characteristics of the different modes of the data are much clearer (Figure 2). The melt component at each location generally has a much lower variance than the ice components due to the soft upper limit of ISTs and the lower truncation point of the model, whereas the ice components have higher variances and more overlap between components. For the sites that experience melt regularly, a substantial proportion of the overall temperature distribution occurs in the overlap between true ice and true melt. A similar result is seen across sites located on or near the coasts, which further validates the decision to use a fixed melt threshold as the melt temperatures - and thereby the melt process - appear to have consistent characteristics across locations.

2.4 Defining melt

Using this model, the probability of melt occurring, which we denote by $\rho(x)$, can be quantified as the ratio of the densities of the ice and melt components. For a given IST x, n_I ice components melt component M, we have:

$$\rho(x) = \frac{f_M(x)}{f_M(x) + \sum_{i=j}^{n_I} f_i(x)}.$$

Consequences of this definition are that for ISTs below $-1.65°$C, the probability of melt is 0, for ISTs above $0°$C the probability of melt is 1, and between these values the melt probability depends on relative values of the melt and ice components' densities.

https://doi.org/10.5194/tc-2021-259
Preprint. Discussion started: 30 August 2021
© Author(s) 2021. CC BY 4.0 License.

For locations with very few or no ISTs above $-1.65°$C, the weight of the melt component may be close to or equal to 0, in which case the probability of melt occurring is effectively zero. Note that there are discontinuities in the model-based estimate of this probability due to the censoring of the mixture components. These discontinuities occur at the edges of the range of interest ($-1.65°$C and $0°$C) and are more or less severe depending on the degree of truncation of the ice and melt components.

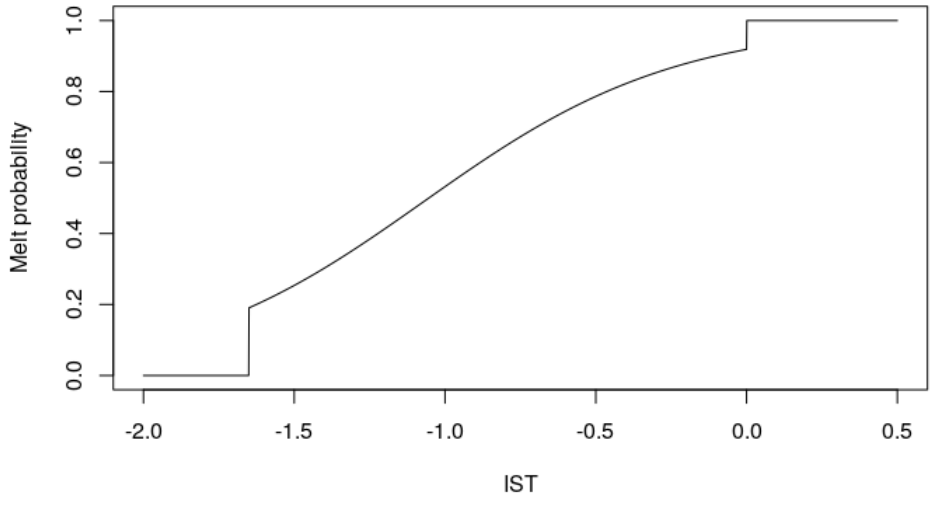

Figure 3. Melt probability estimates of a range of ISTs using the fitted mixture model at a single location (75.37,-58.13) on the Greenland ice sheet between 2001 and 2019. Because some locations have very limited data above $-1.65°$C, we use a location on the west coast with a high proportion of data above $-1.65°$C (22.55%), thus giving us an increased amount of information in the most pertinent temperature range.

3 Results

3.1 Melt extent comparison

Using our model, we calculate the expected number of melt days in each year at each sample location. Let N_y be the number of melt days in year y, then $\mathrm{E}[N_y] = \sum_{i=1}^{m} \rho(x_i)$ where $\rho(x)$ is the notation introduced earlier to denote $\Pr[\text{melt}|X = x]$ and m is the number of observations in year y. The overall annual average is simply the average of the individual annual averages. We then compare our modelled estimates to a simple threshold-based approach to defining melt, i.e. the average number of days per year with temperatures exceeding $-1°$C (Figure 4).

https://doi.org/10.5194/tc-2021-259
Preprint. Discussion started: 30 August 2021
© Author(s) 2021. CC BY 4.0 License.

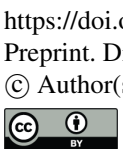

The Cryosphere
Discussions
Open Access
EGU

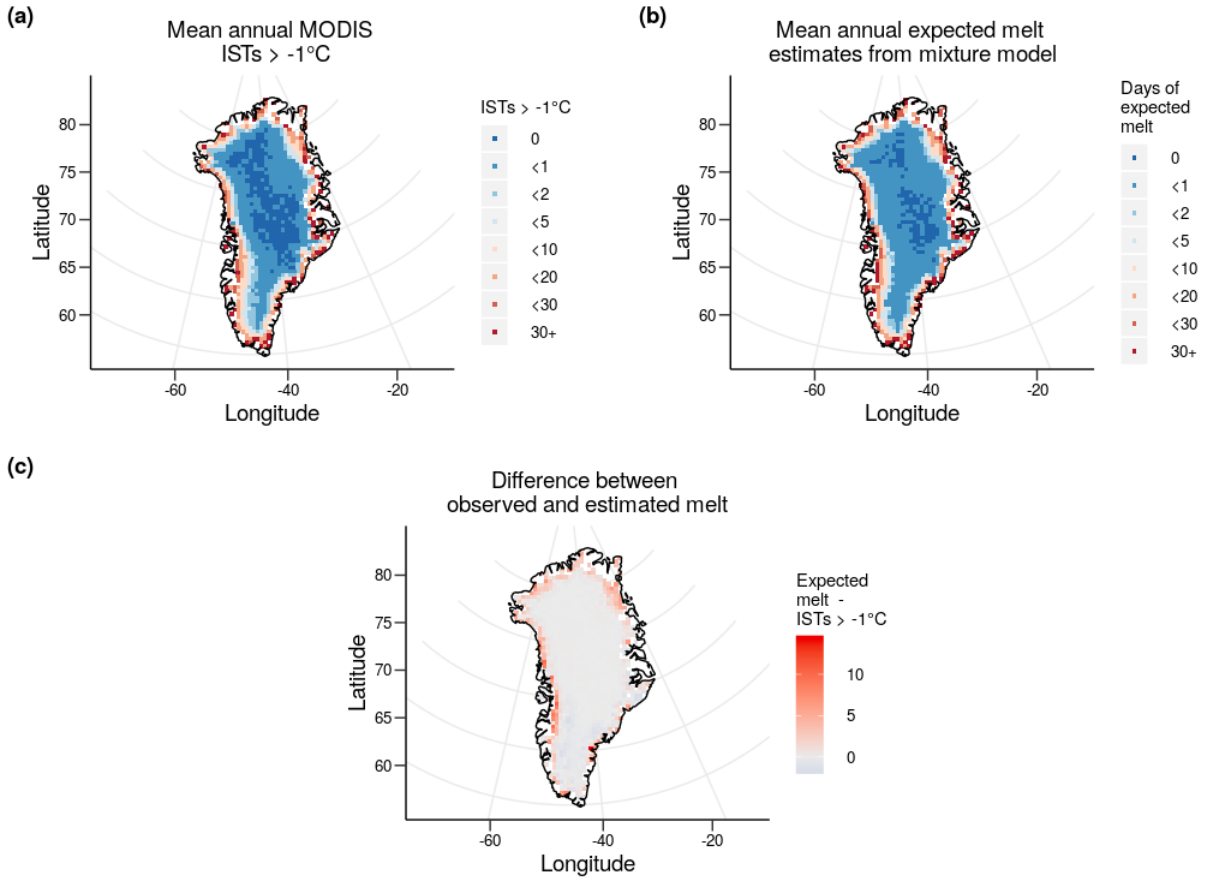

Figure 4. The mean annual number of ISTs above $-1°C$ per year (a), the mean annual expected melt days estimated from each location's mixture model (b), and the difference between the two variables (c).

The majority of the ice sheet - 90.7% of locations from the expected melt from the model, 79.5% from a threshold of $-1°C$ on the data - experiences some degree of melt on average each year, except for sites in the dry snow zone in the centre and north of the ice sheet. Of the locations that experience melt, most (62.2% from the model, 57.3% from the data) sites on average see less than 2 days of melt per year, which makes up the rest of the dry snow zone and most of the percolation zone. The areas with the most melt are located around the coast and in the south and west as may be expected. The main discrepancies between the two measures are at coastal locations, particularly on the west and north coasts. Here, the model estimates a larger amount of melt, with a maximum of 14 additional melt days at 1 specific location on the edge of the south east coast compared to the dataset. However, 89% of locations have an absolute difference of less than 2 melt days, showing the broad agreement between the measures at central locations.

https://doi.org/10.5194/tc-2021-259
Preprint. Discussion started: 30 August 2021
© Author(s) 2021. CC BY 4.0 License.


3.2 Temperature quantiles

We now use the model fit to calculate quantiles of the ISTs at each location (Figure 5). This gives context to the overall temperature trends observed in the dataset, before looking at melt in more detail. We calculate the 90% quantiles to examine the broader trends of high temperatures that aren't necessarily melt temperatures, as well as the 10% quantiles for temperatures that are as relatively low as the 90% quantiles are high. The estimated 10% and 90% quantiles broadly follow the same trends as elevation on the ice sheet. The 10% quantiles have a range from $-53.84°$C in the centre of the ice sheet to a maximum of $-15.75°$C at the south tip of the ice sheet. As would be expected, locations at higher elevations have a lower 10% and 90% quantile. However, of more interest are the few (30/1139) locations located on the west, east and southern coasts that have a 90% quantile above $0°$C. At these locations, we would expect at least (in some cases more than) 10% of observed temperatures to be above $0°$C and thereby melt temperatures.

We also calculate the 1-year return levels of each location. This is the IST that is on average only exceeded once per year as estimated from each location's mixture model. The return levels range from a minimum of $-7.08°$C in the centre to a maximum of $7.24°$C on the west coast. Although, as previously discussed, ISTs should not be seen higher than $0°$C, these return levels reflect similar temperatures recorded by observations in the dataset and can be plausible temperatures when considering the effect that meltwater on the surface of the ice sheet has on the observations. The rarity of melt in certain central areas can be seen more clearly, as temperatures in many locations (519/1139) on average reach $-1.65°$C less than once a year. The trends seen in the return levels also broadly agree with those seen in the quantiles, and are in reasonable agreement with the elevations and distance to the coast of each location, with locations at lower altitudes and closer to the coast generally experiencing more melt.

3.3 Decadal variability

To examine potential changes in melt over time, we fit mixture models at each location for two separate decades: 2001 to 2009 and 2010 to 2019. Averaging over a decade helps to smooth some of the annual variability and thus highlight any potential differences as a result of climatic change. To assess any changes in melt and high ISTs between the decades, we compare quantiles between the fitted models and the estimated melt probabilities at each location in each decade.

3.3.1 Temperature quantiles

Because some central areas of the ice sheet do not have many historical melt observations, we examine the 95% quantiles and yearly expected maximum temperatures, both of which give an indication of overall trends in high temperatures even if these do not reach the level required for melt at some locations. As previously, we take the estimated quantiles from each of the fitted decadal models for each location.

For almost all locations ($1100/1139$), the 95% quantile increased between the two decades. Locations in the south in particular have increased fairly consistently. The average change for all locations south of $73.41°$N was $0.73°$C, with 99.3% of all

https://doi.org/10.5194/tc-2021-259
Preprint. Discussion started: 30 August 2021
© Author(s) 2021. CC BY 4.0 License.

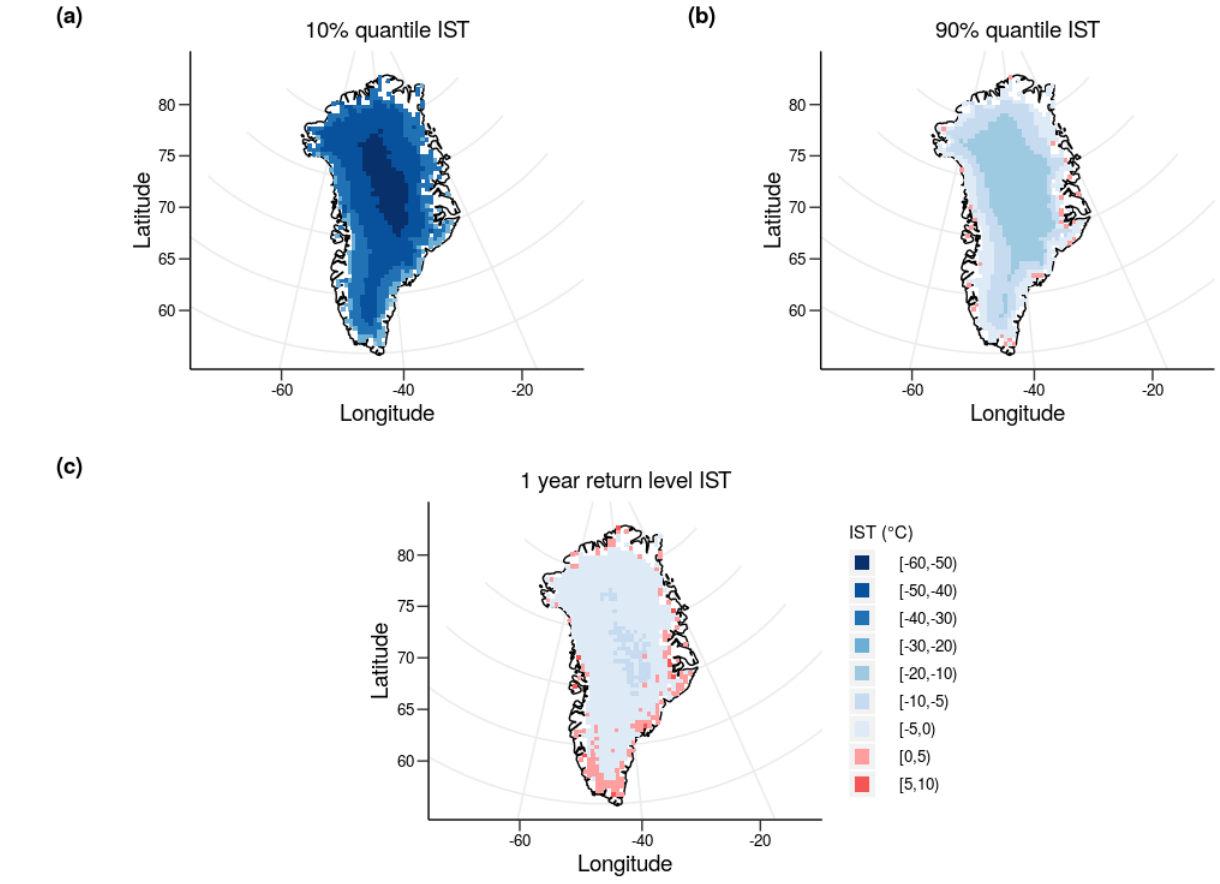

Figure 5. 10% quantile (a), 90% quantile (b), and 1 year return level (c) estimates for MODIS IST data from 2001 to 2019 at 1139 locations. Estimates are calculated from fitted mixture models at each location.

locations further south than this seeing an increase. The largest increases were also concentrated in the southern areas of the ice sheet, with a maximum increase of 1.78°C.

The 1-year return levels also generally increased, albeit slightly less consistently than the 95% quantiles (849/1139 locations). Areas in the east show the largest increases - with the largest increase being 2.66°C - however on the south west coast and particularly the north central area of the ice sheet there are also several locations that show a slight decrease in contrast to larger increases. More clearly than in the 95% quantiles, 1-year return levels at coastal locations do not increase as much as in central locations between decades. However, it is important to note that the maxima at coastal locations are already close to or above 0°C. Because of the soft upper limit of the IST data, values already close to this limit can be partially constrained from further increases, so locations that had a 1-year return level above 0°C are less likely to show an increase than colder areas such as in the centre of the ice sheet. This makes the 1-year return level more informative for central locations than for coastal locations.

https://doi.org/10.5194/tc-2021-259
Preprint. Discussion started: 30 August 2021
© Author(s) 2021. CC BY 4.0 License.

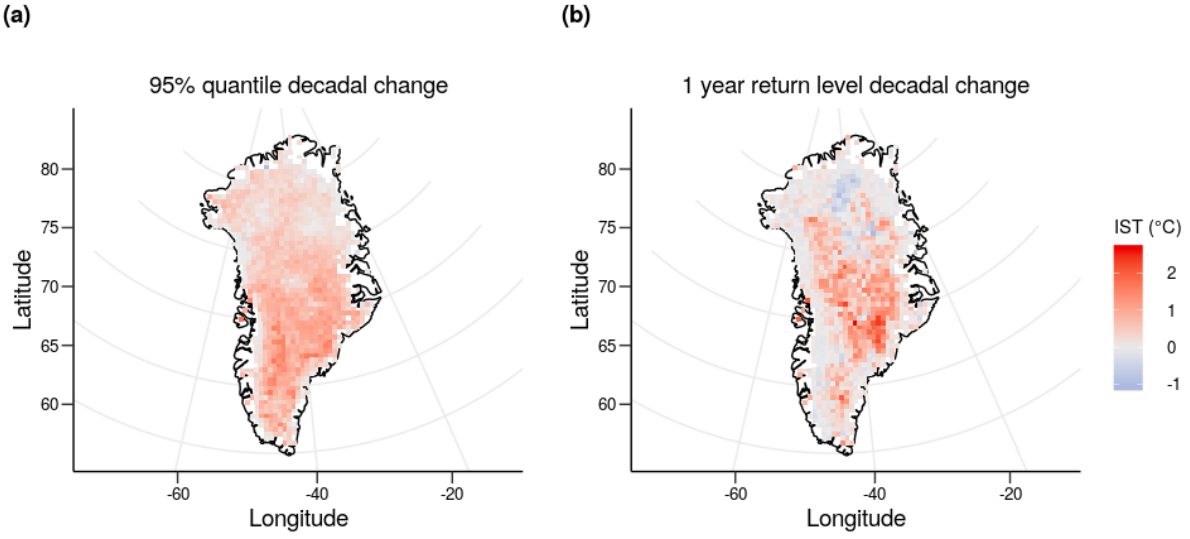

Figure 6. Comparison of the change in 95% quantiles (a) and 1 year return levels (b) of mixture models fit to MODIS IST data from 2001 to 2009 and 2010 to 2019.

3.3.2 Melt probability

We next compare the probability that each location experiences melt on any given day for each decade. Using the fitted models, we estimate the probability that each daily observation is a melt temperature, then take an average of all values within our defined decades. For the purposes of interpretation, we limit our discussions to the summer months (May to September, inclusive) when considering melt probabilities, due to the almost zero probability of observing melt outside of this period.

The two decades show very similar trends in their daily melt probabilities, particularly around the coast. However, decade 2 has more locations with a non-zero probability of melt (1017) than decade 1 (853) - an increase of around 19.2% between the two decades - and 68.5% of locations saw an increased probability of melt between the decades. The location with the single largest probability from either decade is from decade 2 (64.11,-49.93). This location has a probability of a melt temperature on any given summer day of 0.64 - equivalent to an expected 97.92 melt days per year.

Most of central Greenland has experienced minimal change in the probability of melt between the two decades (Figure 7). This may be largely due to the probabilities being extremely small for these areas regardless of the time period chosen. Coastal locations show clearer and larger cross-decadal variation in melt probability. South east and south west areas of the ice sheet were generally more likely to experience melt, in addition to some locations in the north east and north west areas that were less likely to experience melt, in the more recent decade. The largest increase is on the south east coast, where locations show a maximum change of 0.0351, which equates to an expected increase of 15.42 melt days each year.

https://doi.org/10.5194/tc-2021-259
Preprint. Discussion started: 30 August 2021
© Author(s) 2021. CC BY 4.0 License.

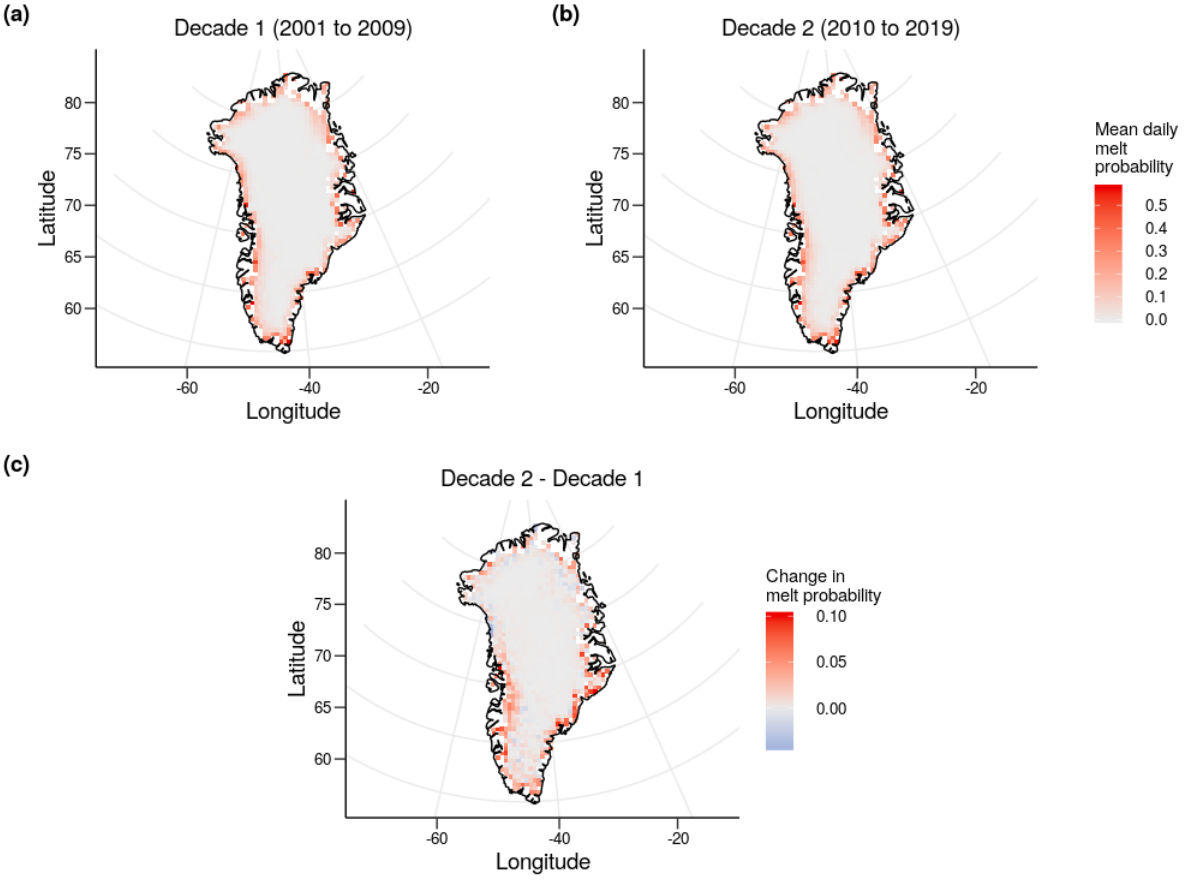

Figure 7. The average probability of a melt temperature on any given summer (May-September inclusive) day from 2001 to 2009 (a) and 2010 to 2019 (b), and the change in melt probability between 2001 to 2009 and 2010 to 2019 calculated from the fitted mixture models.

4 Discussion

Increases in ice melt in Greenland are of major concern due to the impact that it will have on sea levels etc (van den Broeke et al., 2016), however direct observations of ice melt are sparse, discontinuous, and of coarse resolution. Here, we show that melting can be modelled statistically as a function of ISTs. This enables us to assemble a record of melting that is continuous in time and space, and is sampled at high spatial (1km) and temporal (daily) resolution using the MODIS IST dataset. In addition to the greater availability of IST data, ISTs also have characteristics that make them better suited to statistical modelling; in particular, temperatures measured on a continuous scale, and that vary smoothly over time and space. This is of particular interest given that, from these data, we see that there is ambiguity about whether or not temperatures below 0°C are in fact reflective of melting ice. In this paper, we have addressed this uncertainty by incorporating it into the structure of the statistical model, and thus our record of melting/not-melting is probabilistic rather than binary.

https://doi.org/10.5194/tc-2021-259
Preprint. Discussion started: 30 August 2021
© Author(s) 2021. CC BY 4.0 License.


Our model gives comparable results to direct estimation of melt obtained using a fixed threshold, while also allowing more detailed analyses of melt and the overall temperature distribution via quantile estimation, melt probabilities, and return levels. By modelling the entire temperature distribution, not only can we can gain insight into the frequency and range of melt temperatures, but also broader trends such as higher temperatures in both the high and low quantiles.

We observe that melt is much more likely at coastal locations and in the south of the ice sheet than in the centre, and that there is a non-trivial probability of melt occurring below $-1°$C. The spatial melt trends are in keeping with previous work examining melt using surface mass balance data (van den Broeke et al., 2016) and satellite data (Mernild et al., 2011), including MODIS data (Nghiem et al., 2012). The fitted models also show a clear link between elevation and high ISTs similarly to previous studies linking temperature to elevation (Reeh, 1991), and the yearly expected maxima show the potential for even central areas of the ice sheet to experience melt (Nghiem et al., 2012). Trends previously observed in the south (Mote, 2007) also appeared to have continued, as all locations examined south of $75.16°$N saw increases in high-temperature quantiles in the most recent decade.

Although some of the expected annual maxima are just below the lower censoring point of our model's melt component, melt may be possible in these areas over longer time periods. For some locations, the model fit suggests an extremely low probability of melt. This may be because these locations have few historical instances of possible melt in the data, i.e. no ISTs above the lower censoring point of the melt component. In these instances, the information in the data is insufficient to support a melt component, so only the ice components can be fit to the data, leading to an effective zero probability of melt. Given the assumptions and intuition behind some of the modelling choices, this dataset could alternatively be modelled using a Bayesian framework with prior distributions that reflect these assumptions. We would expect melt to have similar distributions at different locations even if there is less evidence of melt in some locations than others. If this is the case, then a modelling framework could be established whereby the melt components of the model share information or parameters, while the ice components are independent between locations. This could be used to estimate melt probabilities even in locations where no melt temperatures have been observed, as melt components could still be estimated using information from other locations with more data resembling melt.

Fitting models to sub-decadal data sets would lead to insufficient data to fit the model; in particular, there would be many locations and time periods with an extremely low number of IST above $-1.65°$C and $0°$C, making it difficult to fit the melt component with any degree of accuracy. By separately fitting the model to data from two decades (2001 to 2009 and 2010 to 2019), the overall temperature trends were examined. South west and south east areas of the ice sheet were found to have a higher probability of melt in 2010 to 2019 compared to 2001 to 2009, and although 22.2% of locations saw a decrease in melt probability of some degree, 68.5% of locations saw an increase in melt probability and the average increase was more than double the average decrease (-0.0044 compared to 0.011). By contrast, the 95% quantiles increased at almost all locations $(1100/1139)$ and the 1-year return levels increased at most locations $(849/1139)$. The overall trends of the model suggest that melt has become more frequent in the most recent decade, and temperatures more broadly are increasing in areas across the ice sheet.

https://doi.org/10.5194/tc-2021-259
Preprint. Discussion started: 30 August 2021
© Author(s) 2021. CC BY 4.0 License.

The Cryosphere Discussions
Open Access
EGU

Appendix A: EM algorithm

A1 Truncated normal distribution

Let $X \sim TN(\mu, \sigma^2, a, b)$ where μ is the mean, σ is the standard deviation, and a (b) is the lower (upper) truncation point. Furthermore, let $\alpha = \frac{a-\mu}{\sigma}$ and $\beta = \frac{b-\mu}{\sigma}$. Then X has probability density function:

$$f_{TN}(x) = \frac{f_N(\frac{x-\mu}{\sigma})}{\sigma(F_N(\beta) - F_N(\alpha))},$$

where f_N and F_N are the probability density function and the cumulative distribution function of a standard normal distribution respectively.

A2 Algorithm

Let $(\mu_k, \sigma_k, \alpha_k, \beta_k)$ denote the parameters for the kth truncated normal distribution. To initialise the algorithm, randomly sample without replacement three values of $x \in X$ and set them as μ_k for $k = 1, 2, 3$. We set $\mu_4 = 0$ to ensure that one of the model components starts in the region of melt temperatures. Let σ_k be the sample variance and the component weights $\phi_k = 1/4$ for $k = 1, 2, 3, 4$. For simplicity we refer to the truncated normal probability density function and cumulative distribution function as $f(x)$ and $F(x)$ respectively. The EM algorithm consists of iterating between two stages, the expectation and maximisation steps, until convergence is obtained. For the expectation step, we set:

$$\hat{\gamma}_{ik} = \frac{\hat{\phi}_k f\left(x_i \mid \hat{\mu}_k, \hat{\sigma}_k\right)}{\sum_{j=1}^{4} \hat{\phi}_j f\left(x_i \mid \hat{\mu}_j, \hat{\sigma}_j\right)}$$

where $\hat{\gamma}_{ik}$ is the estimated probability that observation i belongs to model component k.

For the maximisation step, let:

$$\hat{\phi}_k = \sum_{i=1}^{N} \frac{\hat{\gamma}_{ik}}{N}$$

$$\hat{\mu}_k = \frac{\sum_{i=1}^{N} \hat{\gamma}_{ik} x_i}{\sum_{i=1}^{N} \hat{\gamma}_{ik}} + \hat{\sigma_k} \left(\frac{f(\alpha_k) - f(\beta_k)}{F(\beta_k) - F(\alpha_k)} \right)$$

$$\hat{\sigma}_k^2 = \frac{\sum_{i=1}^{N} \hat{\gamma}_{ik} \left(x_i - \hat{\mu}_k\right)^2}{\sum_{i=1}^{N} \hat{\gamma}_{ik}} \left[1 + \frac{\alpha_k f(\alpha_k) - \beta_k f(\beta_k)}{F_N(\beta) - F_N(\alpha)} - \left(\frac{f(\alpha_k) - f(\beta_k)}{F_N(\beta) - F_N(\alpha)} \right)^2 \right].$$

We iterate between these two steps until the parameters converge to the final estimates (800 iterations was sufficient in this case). The algorithm is considered to have converged if the difference between parameters in each iteration is sufficiently small. We found a difference of 10^{-5} between iterations to be sufficient indication of convergence for all parameters.

Author contributions. DC and EE devised the model framework and carried out the data analysis. DC, EE, and AL worked on the interpretation of the model and results and wrote the manuscript.

https://doi.org/10.5194/tc-2021-259
Preprint. Discussion started: 30 August 2021
© Author(s) 2021. CC BY 4.0 License.

Competing interests. The authors declare that they have no conflict of interest.

Acknowledgements. This work was supported by the Data Science for the Natural Environment project (EPSRC grant number EP/R01860X/1).

https://doi.org/10.5194/tc-2021-259
Preprint. Discussion started: 30 August 2021
© Author(s) 2021. CC BY 4.0 License.

References

Chen, X., Zhang, X., Church, J. A., Watson, C. S., King, M. A., Monselesan, D., Legresy, B., and Harig, C.: The increasing rate of global mean sea-level rise during 1993–2014, Nature Climate Change, 7, 492–495, https://doi.org/10.1038/nclimate3325, number: 7 Publisher: Nature Publishing Group, 2017.

Fettweis, X., Tedesco, M., Broeke, M. v. d., and Ettema, J.: Melting trends over the Greenland ice sheet (1958–2009) from spaceborne microwave data and regional climate models, The Cryosphere, 5, 359–375, https://doi.org/https://doi.org/10.5194/tc-5-359-2011, 2011.

Hall, D., Key, J., Casey, K., Riggs, G., and Cavalieri, D.: Sea ice surface temperature product from MODIS, IEEE Transactions on Geoscience and Remote Sensing, 42, 1076–1087, https://doi.org/10.1109/TGRS.2004.825587, 2004.

Hall, D., Box, J., Casey, K., Hook, S., Shuman, C., and Steffen, K.: Comparison of satellite-derived and in-situ observations of ice and snow surface temperatures over Greenland, Remote Sensing of Environment, 112, 3739–3749, https://doi.org/10.1016/j.rse.2008.05.007, 2008.

Hall, D. K. and DiGirolamo, N.: Multilayer Greenland Ice Surface Temperature, Surface Albedo, and Water Vapor from MODIS, Version 1, https://doi.org/https://doi.org/10.5067/7THUWT9NMPDK, Boulder, Colorado USA. NASA National Snow and Ice Data Center Distributed Active Archive Center, 2019.

Hanna, E., Fettweis, X., Mernild, S. H., Cappelen, J., Ribergaard, M. H., Shuman, C. A., Steffen, K., Wood, L., and Mote, T. L.: Atmospheric and oceanic climate forcing of the exceptional Greenland ice sheet surface melt in summer 2012, International Journal of Climatology, 34, 1022–1037, https://doi.org/10.1002/joc.3743, 2014.

Koenig, L. S. and Hall, D. K.: Comparison of satellite, thermochron and air temperatures at Summit, Greenland, during the winter of 2008/09, Journal of Glaciology, 56, 735–741, https://doi.org/10.3189/002214310793146269, 2010.

Mernild, S. H., Mote, T. L., and Liston, G. E.: Greenland ice sheet surface melt extent and trends: 1960–2010, Journal of Glaciology, 57, 621–628, https://doi.org/10.3189/002214311797409712, publisher: Cambridge University Press, 2011.

Mote, T. L.: Greenland surface melt trends 1973–2007: Evidence of a large increase in 2007, Geophysical Research Letters, 34, https://doi.org/https://doi.org/10.1029/2007GL031976, _eprint: https://agupubs.onlinelibrary.wiley.com/doi/pdf/10.1029/2007GL031976, 2007.

Mouginot, J., Rignot, E., Bjørk, A. A., Broeke, M. v. d., Millan, R., Morlighem, M., Noël, B., Scheuchl, B., and Wood, M.: Forty-six years of Greenland Ice Sheet mass balance from 1972 to 2018, Proceedings of the National Academy of Sciences, 116, 9239–9244, https://doi.org/10.1073/pnas.1904242116, publisher: National Academy of Sciences Section: Physical Sciences, 2019.

Nghiem, S. V., Hall, D. K., Mote, T. L., Tedesco, M., Albert, M. R., Keegan, K., Shuman, C. A., DiGirolamo, N. E., and Neumann, G.: The extreme melt across the Greenland ice sheet in 2012, Geophysical Research Letters, 39, https://doi.org/10.1029/2012GL053611, 2012.

Reeh, N.: Parameterization of Melt Rate and Surface Temperature in the Greenland Ice Sheet, https://epic.awi.de/id/eprint/28262/, iSSN: 0032-2490 Issue: 3 Number: 3 Pages: 113-128 Place: Bremerhaven Publisher: Alfred Wegener Institute for Polar and Marine Research & German Society of Polar Research Volume: 59, 1991.

Rignot, E., Velicogna, I., Broeke, M. R. v. d., Monaghan, A., and Lenaerts, J. T. M.: Acceleration of the contribution of the Greenland and Antarctic ice sheets to sea level rise, Geophysical Research Letters, https://doi.org/10.1029/2011GL046583@10.1002/(ISSN)1944-8007.GRL40, 2018.

Smith, D. M., Cusack, S., Colman, A. W., Folland, C. K., Harris, G. R., and Murphy, J. M.: Improved Surface Temperature Prediction for the Coming Decade from a Global Climate Model, Science, 317, 796–799, https://doi.org/10.1126/science.1139540, publisher: American Association for the Advancement of Science Section: Report, 2007.

https://doi.org/10.5194/tc-2021-259
Preprint. Discussion started: 30 August 2021
© Author(s) 2021. CC BY 4.0 License.


Tedesco, M., Fettweis, X., Mote, T., Wahr, J., Alexander, P., Box, J., and Wouters, B.: Evidence and analysis of 2012 Greenland records from spaceborne observations, a regional climate model and reanalysis data, Cryosphere (The), 7, https://doi.org/10.5194/tc-7-615-2013, 2013.

van den Broeke, M. R., Enderlin, E. M., Howat, I. M., Kuipers Munneke, P., Noël, B. P. Y., van de Berg, W. J., van Meijgaard, E., and Wouters, B.: On the recent contribution of the Greenland ice sheet to sea level change, The Cryosphere, 10, 1933–1946, https://doi.org/10.5194/tc-10-1933-2016, publisher: Copernicus GmbH, 2016.

Vermeer, M. and Rahmstorf, S.: Global sea level linked to global temperature, Proceedings of the National Academy of Sciences, 106, 21 527–21 532, https://doi.org/10.1073/pnas.0907765106, 2009.

Zhengming, W. and Dozier, J.: Land-surface temperature measurement from space: physical principles and inverse modeling, Geoscience and Remote Sensing, IEEE Transactions on, 27, 268–278, https://doi.org/10.1109/36.17668, 1989.